ISSN 1573-160X, *PHYSICAL OCEANOGRAPHY*, Vol. 30, Iss. 5, pp. 581-593 (2023)
Original Russian Text © V. L. Dorofeev, L. I. Sukhikh, 2023,
published in *Morskoy Gidrofizicheskiy Zhurnal*, 2023, Vol. 39, Iss. 5, pp. 617–630.

Original article

Analysis of Long-Term Variability of Hydrodynamic Fields in the Upper 200-Meter Layer of the Black Sea Based on the Reanalysis Results

V. L. Dorofeev, L. I. Sukhikh ✉

Marine Hydrophysical Institute of RAS, Sevastopol, Russian Federation
✉ *l.sukhikh@gmail.com*

Abstract

Purpose. The research is purposed at studying the trends in the long-term evolution of hydrodynamic fields in the upper 200-m layer of the Black Sea based on the reanalysis of a 28-year period.

Methods and Results. To obtain a set of the Black Sea hydrodynamic fields for the period from 1993 to 2020, the following calculations were performed using the MHI numerical model of the Black Sea and including the assimilation of remote sensing data: the anomaly fields of the free sea surface elevation and the surface temperature derived from satellite measurements. The results of the ERA-5 atmospheric reanalysis were used as the atmospheric forcing. The evolution of temperature, salinity and current fields in the sea upper layers over the period under consideration was analyzed. The modeling results were compared to the temperature and salinity profiles obtained by the ARGO buoys in the Black Sea.

Conclusions. The results obtained demonstrate the positive trends in average temperature in different layers, an increase of heat content of the sea upper layer and a growth of average temperature in the core of the cold intermediate layer. In course of the period under study, salinity also tended to increase.

Keywords: reanalysis, circulation model, Black Sea, numerical modeling, assimilation of measurement data, satellite data

Acknowledgments: The study was carried out with the financial support of project No. 0827-2021-0002.

For citation: Dorofeev, V.L. and Sukhikh, L.I., 2023. Analysis of Long-Term Variability of Hydrodynamic Fields in the Upper 200-Meter Layer of the Black Sea Based on the Reanalysis Results. *Physical Oceanography*, 30(5), pp. 581-593.

Introduction

To restore the condition of hydrodynamic fields of oceans and seas for a certain period in the past, the method of retrospective analysis (reanalysis) is widely used. Reanalysis is based on the observational data assimilation in a numerical hydrodynamic model and permits to monitor the marine environment state and its evolution. Although numerical models are powerful tools for studying three-dimensional water circulation in an ocean or other water basin, they cannot fully monitor the basin state. For monitoring tasks, the observational data assimilation into a hydrodynamic model is of crucial importance.

One of the first studies on reanalysis of the Black Sea state are works in which the seasonal and interannual variability of the hydrodynamic Black Sea fields is simulated based on the assimilation of hydrological measurements for the periods from 1985 to 1994 [1] and from 1973 to 1993 [2]. Recently, remote sensing data has become widespread, providing wide coverage of the water area and uninterrupted data flow. In [3], the results of a reanalysis of the hydrodynamic

Black Sea fields for 1992–2002 are given. This reanalysis was carried out based on the same hydrodynamic model that was used in [1, 2] (ROM model), but using satellite altimetry data assimilation.

The reanalysis result is a temporal set of three-dimensional hydrological and current fields on a regular grid used to analyze temporal variability. In addition, the reanalysis results are used as input parameters in modeling the state and dynamics of marine ecosystems [3, 4], as well as in solving other applied problems.

The present paper presents some results of the long-term evolution of the hydrodynamic Black Sea fields obtained on the basis of a reanalysis carried out over a 28-year period (1993–2020). The choice of this period is explained by the fact that since 1993, satellite altimetry measurements have become available and their assimilation plays a significant role in the reconstruction of sea currents. The presented results add to those previously obtained from reanalysis for the 1993–2012 period [5].

Data and methods

The Black Sea circulation model

As noted above, the reanalysis central element is the numerical model. In this study, the Black Sea circulation model of MHI built on the approximation of a system of primitive ocean dynamics equations was taken as a basis [6]. A model version with a spatial step of 4.8 km was used, which permitted to describe adequately both large-scale circulation and synoptic processes. Vertically, the model contains 35 calculated z-levels compressed towards the sea surface. To parameterize vertical turbulent diffusion and viscosity, coefficients that depend on depth and seasonally on time are used. To calculate penetrating solar radiation, climatic attenuation coefficients obtained from an optical model, are used [7]. At the estuaries of large rivers, climatic values of flow rates were specified [8]. Previously, this version of the circulation model was used in the nowcast/forecast system of the Black Sea hydrophysical fields [9]. To take into account water exchange through the Bosporus at horizons corresponding to the Lower Bosporus Current, velocities determined by climatic flow and a salinity value of 36‰ were set. At the horizons corresponding to the Upper Bosporus Current, where water flows out of the Black Sea, a constant velocity value ensuring the water balance for the studied time period, was set.

Atmospheric forcing

To set the boundary conditions on the free sea surface for the circulation model equations, the atmospheric fields of surface wind, heat and fresh water flows, and solar radiation obtained from the ERA-5 atmospheric reanalysis (ECMWF) results [10], were used. The spatial resolution of atmospheric fields is 0.25° × 0.25°, the time frequency is 1 hour.

Data for assimilation

The Black Sea circulation model assimilated satellite measurements of sea surface temperature (SST), altimetry data, and mean annual temperature and

salinity profiles. Surface temperature was a CMEMS-prepared daily dataset on a regular grid with a spatial resolution of 0.05° × 0.05°. Altimetry data (CMEMS) were L4 sea level anomalies (SLA) on a regular grid (0.15° × 0.15°) calculated with respect to the 20-year mean (from 1993 to 2012). SLAs were calculated using optimal interpolation combining along-track L3 measurements from various available altimeter missions [11].

For assimilation in the circulation model, level anomalies were converted to free surface elevation. For this purpose, the mean dynamic topography calculated based on the results of the previous version of the reanalysis (1993–2012) [5], was used. Mean annual temperature and salinity profiles were prepared based on all available hydrographic surveys and ARGO buoys data for the period under review.

Assimilation of sea surface temperature was carried out by the relaxation method. Satellite SST values were compared with model surface temperature values once a day. At the measurement points on the model horizons included in the upper mixed layer, sources were included on the right side of the heat advection-diffusion equation, proportional to the discrepancy of temperature values.

To assimilate satellite altimetry data, the algorithm described in [12] was used. Temperature and salinity profiles were adjusted at each point in proportion to the difference between the measured free sea surface elevation and the model value. In this case, depth-dependent weighting coefficients were calculated using cross-covariance functions of level and salinity and/or temperature.

Depth-average temperature and salinity values were corrected at horizons below 500 m in accordance with the mean annual profiles obtained from all available contact measurement data.

Results

The reanalysis results accuracy estimation

The quality of the reanalysis products was assessed by comparing the results obtained with temperature and salinity profiles measured by ARGO buoys drifting in the Black Sea during the considered period [13]. For comparison with measurement data, the temperature and salinity fields obtained in the reanalysis were interpolated to the measurement points with ARGO floats. After this, the average and standard deviations of the measured values from the model values were calculated for the entire array of measurements at the calculated horizons of the circulation model. To eliminate large outliers in the measurement data, control was carried out using the criterion of anomalies exceeding the average 3σ.

Fig. 1 shows profiles of average and standard deviations of measurement data from model values of temperature and salinity at the calculated horizons of the circulation model.

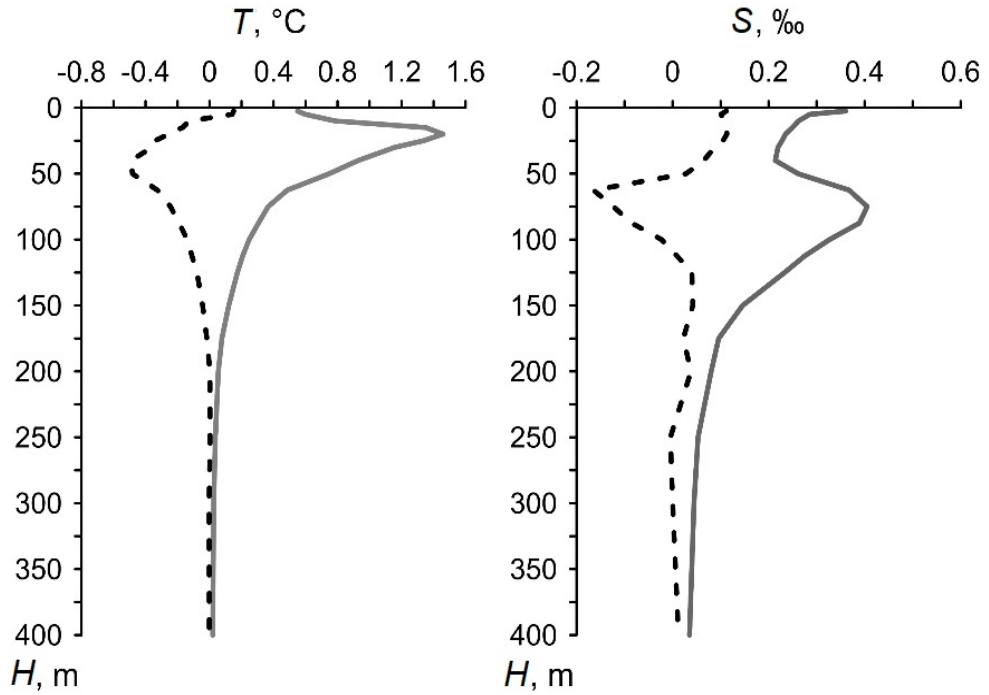

F i g. 1. Profiles of the average (dashed line) and standard (solid line) deviations of measurement data from the reanalysis results for temperature (*left*) and salinity (*right*)

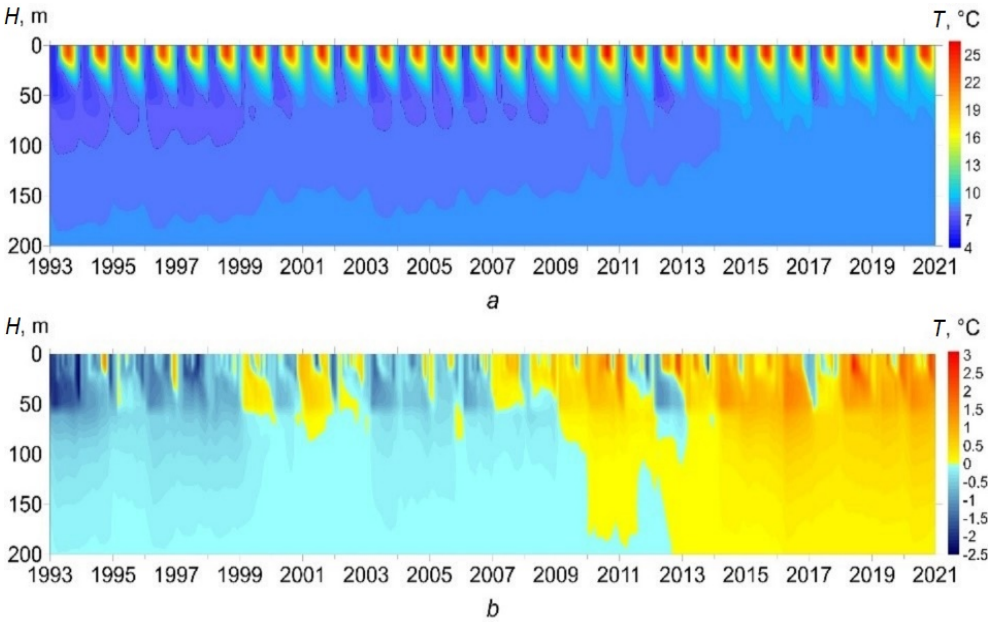

F i g. 2. Evolution of the temperature (*a*) and temperature anomalies (*b*) average over the basin area in the upper 200-m layer of the Black Sea

The standard deviation of the model temperature from the measured one has a maximum at the horizon of approximately 25 m. This maximum corresponds to the summer seasonal thermocline position characterized by a large temperature gradient. Therefore, even small errors in determining the thermocline position lead to large errors. The largest deviation of the average profiles is observed at a depth of about 50 m, where the average model values exceed the measurements by ~ 0.5 °C. The cold intermediate layer (CIL) core is located approximately at this depth (Fig. 2). The excess of the model temperature over the measured one can be caused by warmer CIL waters in the model. In addition, the lower boundary of the mixed layer in winter is located approximately at this depth. Error in the determination of this boundary by the model can also contribute to temperature bias.

For salinity, the maximum errors, both systematic and root mean square, are located at depths of approximately 60–80 m, that is, in the halocline location. In this case, the maximum mean overestimation of salinity in this layer by the model is 0.2‰. At the surface, the systematic error is 0.1‰. The water salinity obtained from the modeling results is lower than that from the measurement results. The standard deviation of salinity has a second maximum on the surface, which is slightly less than the maximum in the halocline.

Temperature trends in the upper sea layer

Below, the trends in water temperature changes in the Black Sea upper layer are considered. To analyze long-term and seasonal variability, we will study monthly mean fields.

Fig. 2 shows the Hovmöller diagrams for the average temperature values over the basin area and its anomalies. The anomalies were determined in relation to climatic values calculated by averaging over the entire reanalysis period (28 years). The temperature diagram shows a clear seasonal signal. In addition, the warming of water in the upper 200-meter layer is clearly visible. The solid blue line marks the area with temperatures below 8 °C, which is one of the CIL indicators used in the Black Sea [14]. In the 1990s, this area was observed to a depth of about 100 m and even deeper. Then it decreased and almost never observed in the 2010s. In the diagram for temperature anomalies, the heating of the upper sea layer is manifested in the fact that in the second half of the studied period the anomalies are mostly positive, while in the first half they are negative, except for 1999 and 2001.

To quantify the heating of the Black Sea upper layer, Fig. 3 shows the graphs of changes in average temperature in three layers: 0–30 m, 30–150 m, and 150–300 m, and linear trends in temperature changes over the considered period. In the 0–30 m layer, seasonal fluctuations are the main element of temporal variability. In the 30–150 m layer, they are also visible, but have a smaller amplitude, and in the 150–300 m layer, seasonal fluctuations are almost not observed. The temperature trend estimated over the entire period under consideration is as follows for three layers: (0.084 ± 0.032) °C/year,

(0.047 ± 0.0023) °C/year, and (0.0083 ± 0.0002) °C/year, respectively. By comparison, the values of temperature trends obtained in [15] are given. This paper also examines the Black Sea reanalysis results, but for the 1993–2018 period. For the 0–25 m layer, the linear trend was 0.0829 °C/year, for the 25–150 m layer – 0.038 °C/year, and for the 150–300 m layer – 0.0041 °C/year.

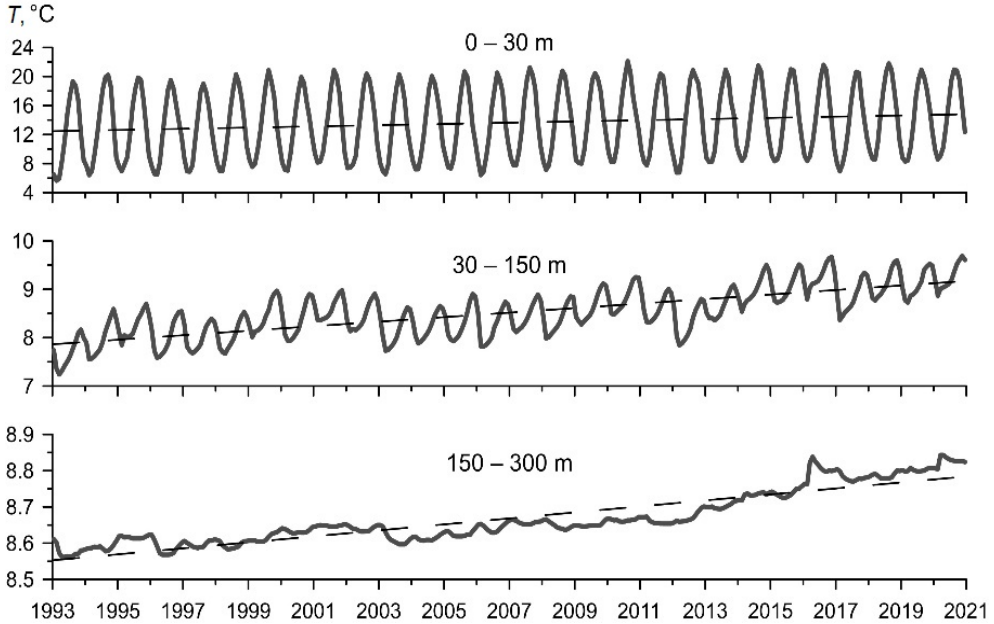

F i g. 3. Temporal evolution of average temperature in three layers (solid line) and linear trends (dashed line)

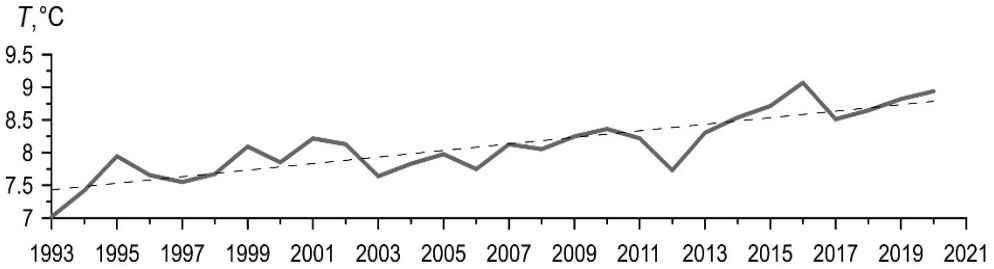

F i g. 4. Temporal evolution of average temperature in the CIL core for the period May – October (solid line), temperature trend (dashed line)

As noted before, water masses with water temperatures below 8 °C are the generally accepted CIL indicator in the Black Sea. Fig. 2 shows that for almost half of the period under consideration, areas with temperatures below 8 °C are not observed practically. Analysis of the results showed that during the specified period of time, the CIL also exists, but the temperature in it is higher than 8 °C. Fig. 4 shows the average temperature of the CIL core for May – October. This

value was calculated by averaging the temperature values over the area and the specified time period at the minimum point of the temperature profiles. This figure also shows clearly the warming of the Black Sea upper layer. The linear temperature trend is 0.05 °C/year, which almost coincides with the linear trend for the entire 30–150 m layer, in which the CIL is located.

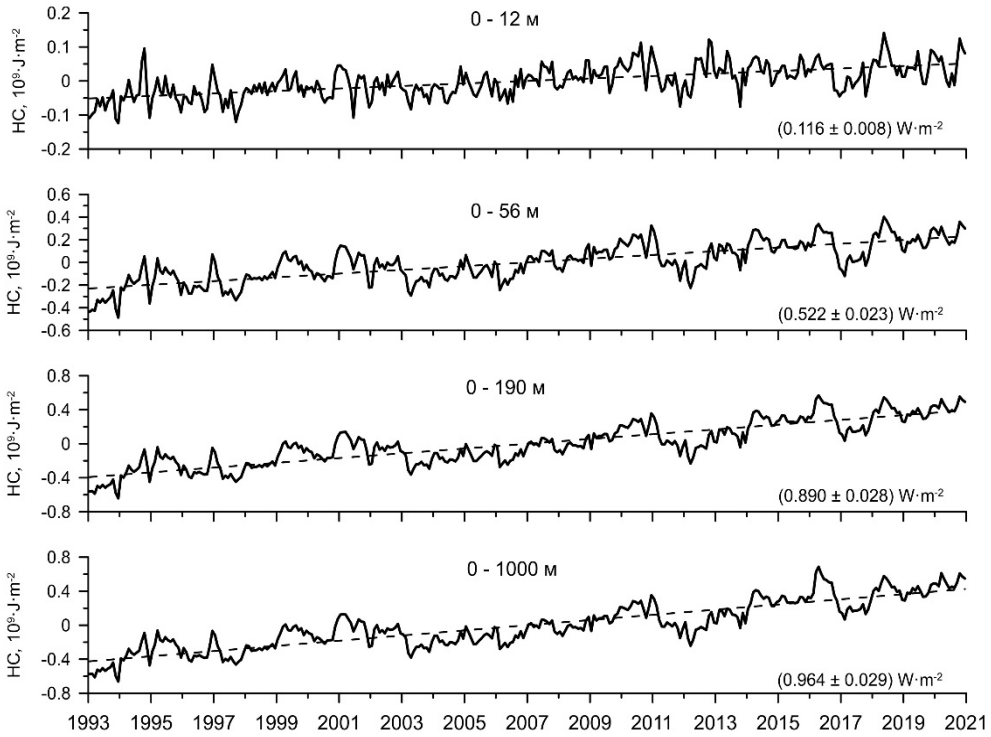

F i g. 5. Changes in the deviation of seawater heat content (HC) from the climatic one and the value of its trend for different layers

Another quantity characterizing the thermodynamics of the upper layer is its heat content (HC). Following the work [16], the sea layer HC is determined by the following formula:

$$HC = \rho_0 C_p \int_{z_1}^{z_2} (T - T_{cl}) dz, \qquad (1)$$

where $\rho_0 = 1020$ kg/m^3 is the density; $C_p = 4181.3$ J/(kg·°C) is the specific heat capacity of sea water; T is the temperature; T_{cl} is the climatic temperature obtained for the entire period under consideration; z_1 and z_2 are the layer boundaries. That is, formula (1) determines the deviation of the sea water layer HC from the climatic one. Fig. 5 shows graphs of changes in this value for different layers. A positive trend is observed for all layers. In the 0–12 m layer, with a general positive trend, peaks of maxima and minima are observed. At the end of 1994 and 1996,

the largest positive HC values are observed in the form of peaks on the graph, although in general, the heat reserve values in the vicinity of these peaks are negative. At this time, the diagram (see Fig. 2) shows positive water temperature anomalies near the surface against the background of negative temperature anomalies. The most significant peaks of negative values of heat storage anomalies correspond to the end of 2011 – beginning of 2012, the end of 2013, and the end of 2016 – beginning of 2017. During these intervals, the diagram (see Fig. 2) shows negative temperature anomalies against the background of generally positive ones clearly.

Salinity

Fig. 6 shows diagrams of changes in depth and time of salinity values and salinity anomalies averaged over the basin area similar to diagrams for temperature (see Fig. 2). Seasonal variability is clearly visible up to a depth of about 60 m. Then the seasonal signal weakens. In the interannual variability, for approximately half of the time period under consideration, salinity anomalies are negative throughout the entire 200-meter layer. The exception is the upper 60-meter layer during the first four years. In the second half, salinity anomalies are mostly positive. That is, throughout the entire period under consideration, salinity in the upper 200-meter layer of the Black Sea tends to increase.

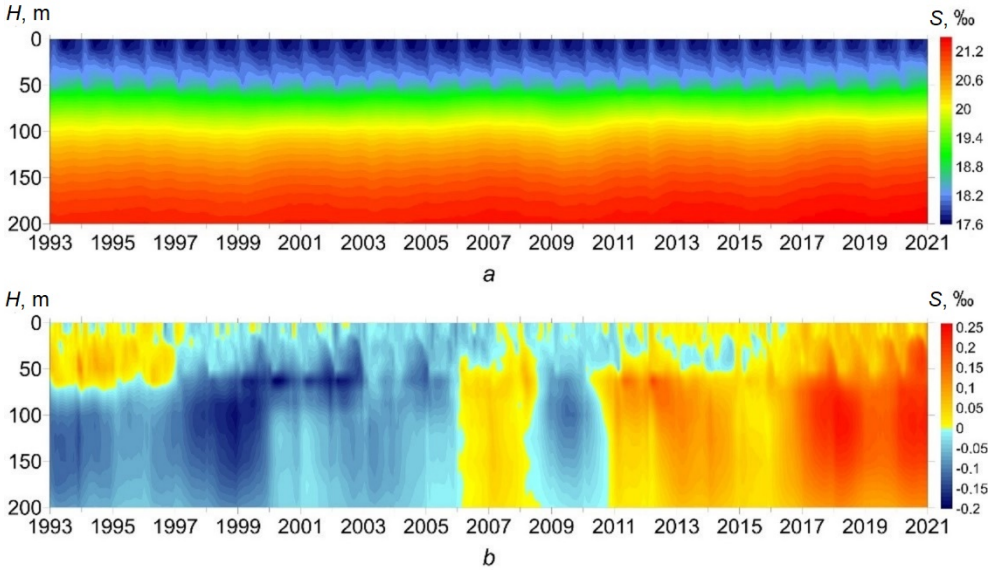

F i g. 6. The Hovmöller diagrams for the salinity (*a*) and salinity anomalies (*b*) average over the basin area

Fig. 7 shows graphs of changes in average salinity values in the layers: 0–30, 30–150, and 150–300 m. The dashed line shows linear trends. Despite the fact that salinity decreases in the 0–30 m layer until approximately 2003, in general, over

the entire period under consideration, linear trends are positive for all three layers. For the 0–30 m layer, it has a value of (0.002 ± 0.0005) ‰/year, for the 30–150 m layer – (0.009 ± 0.0004) ‰/year, and for the 150–300 m layer – (0.007 ± 0.00016) ‰/year. In [15], for the 0–25 m layer, the linear trend was 0.0068 ‰/year, for the 25–150 m layer – 0.0062 ‰/year, and for the 150–300 m layer – 0.0029 ‰/year. Thus, our study shows that the salinization of surface waters occurs more slowly (in comparison with the results obtained in [15]), and in deeper layers it occurs faster.

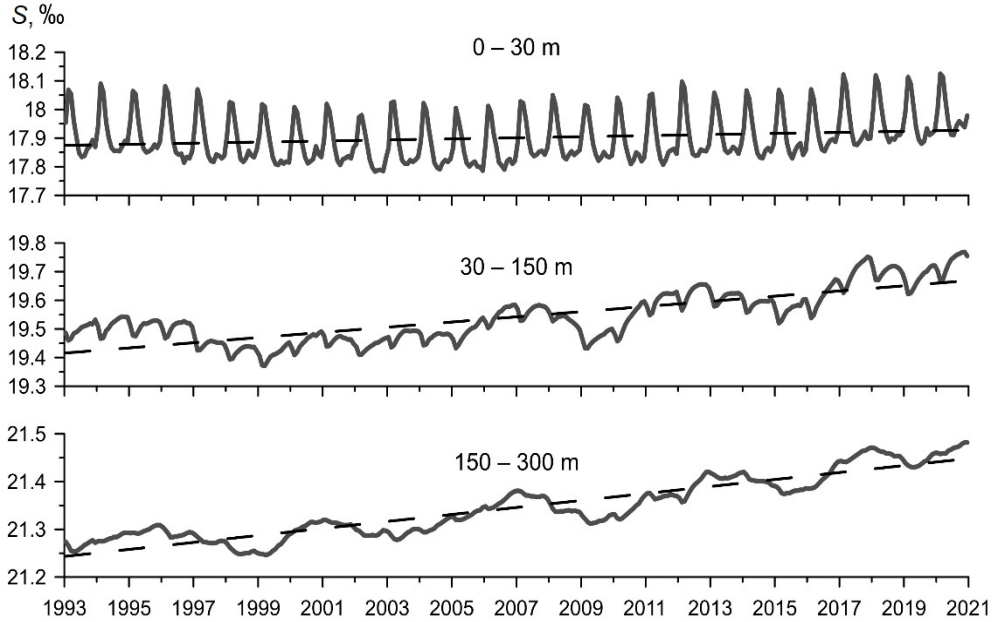

F i g. 7. Temporal evolution of average salinity in three layers (solid line) and linear trends (dashed line)

In [17], graphs of salinity and temperature changes in the Black Sea upper layer, obtained at stations with a depth of 500 m in the area of Gelendzhik, are presented. The behavior of salinity in the 0–25 m layer corresponds qualitatively to that shown in Fig. 7 in the 0–30 m layer. Until about 2009, salinity decreases, then increases. In the layer up to 150 m, an increase in salinity is also observed. In addition, according to this paper, the temperature of the upper sea layer has been increasing since 2010, which is also consistent with the results of the present study.

Circulation

Fig. 8 shows maps of the monthly mean climatic circulation in the upper 30-meter layer along with the Black Sea free surface elevation. The main element of circulation in the upper layer is the Black Sea Rim Current, which forms a cyclonic gyre. It is accompanied by reduced free surface elevation values in the central part of the basin. In addition to the two main level minima in the first six months of

the year, the third minimum is observed in the eastern Black Sea. It then merges with the main eastern sea level low and appears in December.

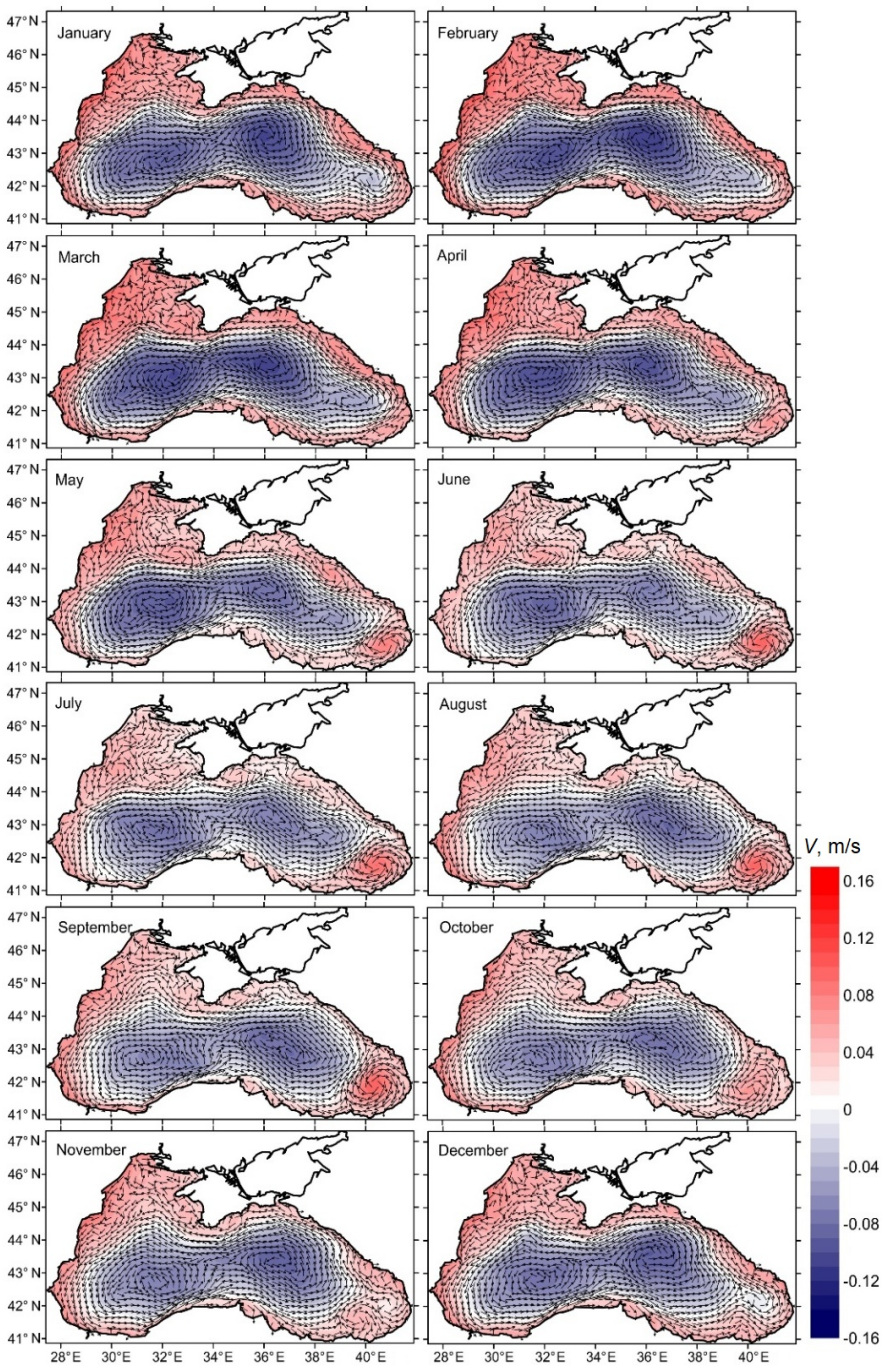

F i g. 8. Maps of monthly average climatic circulation in the upper 30-m layer of the Black Sea (arrows). Color shows the free surface elevation

Another important circulation element is the Batumi anticyclonic gyre. It appears in April and is most pronounced during the summer months. In summer, peripheral anticyclones are also visible near the coast of Crimea and the Caucasus. In November, a small anticyclone remains from the Batumi gyre, pressed against the southern coast, and it disappears in December. The behavior of the current along the west coast on the northwestern shelf is also interesting. In winter, it is directed mainly to the south, and in the summer months – in the opposite direction. The change in the direction of the current integrated over the 30 m layer is explained by the presence of a northward-directed current at a depth of approximately 20 m caused by strong horizontal stratification (for more details, see [18]).

The change in current intensity in the upper 30-meter layer over the period under consideration is shown in Fig. 9 in the form of graphs of the time dependence of the average kinetic energy density in the layer and its deviations from the climate.

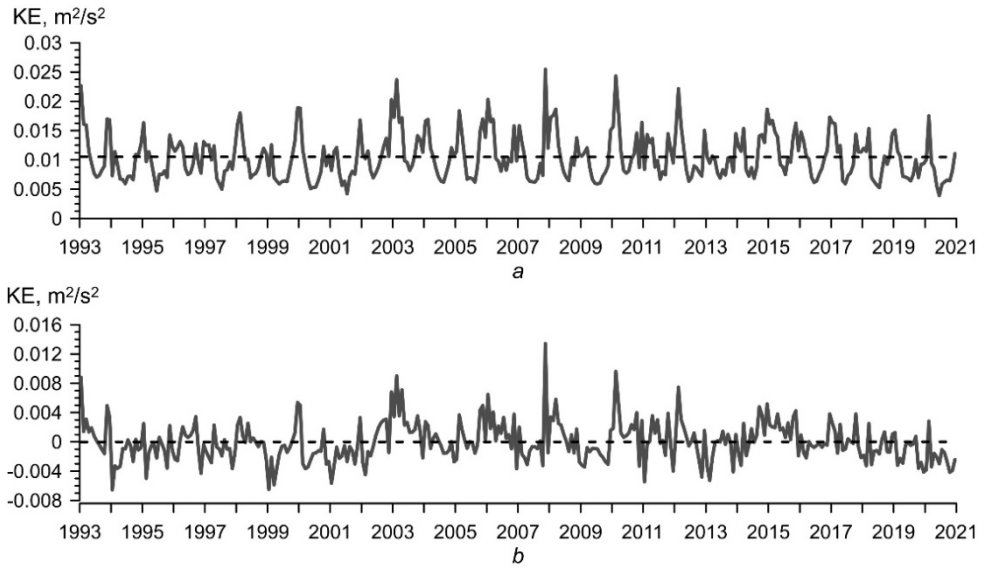

F i g. 9. Monthly average kinetic energy density in the upper 30-m layer of the Black Sea (*a*) and its deviation from the climatic values (*b*). Dashed lines show the linear trends

The seasonal variation of kinetic energy density is visible clearly. Its maxima occur in the winter season, when the strongest winds are observed over the Black Sea. Interannual variability is also clearly visible, especially in winter, which is manifested in large deviations from climate in the graph (Fig. 9). If the long-term trend is considered, then, in contrast to salinity and temperature, the value of the linear trend for the kinetic energy density is almost zero.

Conclusion

Analysis of the 28-year evolution of hydrological fields and current fields of the Black Sea obtained on the basis of the assimilation of satellite measurements of free surface elevation and surface temperature shows trends in heating and

salinization of the upper sea layer. Temperature variation graphs in three upper layers have positive linear trends. The average temperature anomalies over the basin area relative to climatic values in the upper 200-meter layer have mostly negative values until 2010 and positive values until the end of the period under consideration. The heating of the Black Sea upper layer is also confirmed by the positive trend in the change in heat content in the 1000-meter layer and increase in the CIL average temperature.

Salinity in the Black Sea upper layer also has a positive growth trend over the entire period. But if the period before 2005 is considered, then in the upper 30-meter layer the salinity decreases, which can be seen in the salinity variation graph in this layer.

The climatic picture of currents in the upper 30-meter layer of the Black Sea constructed based on the reanalysis results generally reflects the main elements of circulation: the Black Sea Rim Current, the Batumi anticyclonic gyre, and peripheral anticyclonic eddies near the coast of Crimea and the Caucasus. The Batumi gyre appears in March – April and disappears in November. The average longshore current in the 30-meter layer on the northwestern shelf is directed south in winter and changes direction to the opposite in summer. The variability of the kinetic energy density of currents in the upper sea layer has a pronounced seasonal and interannual character, but no noticeable trend is observed over the period under consideration.

REFERENCES

1. Knysh, V.V., Kubryakov, A.I., Moiseenko, V.A., Belokopytov, V.N., Inyushina, N.V. and Korotaev, G.K., 2008. Tendencies of Variability of the Black Sea Thermohaline and Dynamic Parameters, Revealed by Reanalysis Results for the 1985–1994 Years Period. In: MHI, 2008. *Ekologicheskaya Bezopasnost' Pribrezhnoy i Shel'fovoy Zon i Kompleksnoe Ispol'zovanie Resursov Shel'fa* [Ecological Safety of Coastal and Shelf Zones and Comprehensive Use of Shelf Resources]. Sevastopol: MHI. Iss. 16, pp. 279-290 (in Russian).
2. Knysh, V.V., Korotaev, G.K., Moiseenko, V.A., Kubryakov, A.I., Belokopytov, V.N. and Inyushina, N.V., 2011. Seasonal and Interannual Variability of Black Sea Hydrophysical Fields Reconstructed from 1971–1993 Reanalysis Data. *Izvestiya, Atmospheric and Oceanic Physics*, 47(3), pp. 399-411. doi:10.1134/S000143381103008X
3. Dorofeev, V.L., 2009. Modeling of Decadal Variations in the Black-Sea Ecosystem. *Physical Oceanography*, 19(6), pp. 400-409. doi:10.1007/s11110-010-9062-6
4. Dorofeev, V.L., Korotaev, G.K. and Sukhikh, L.I., 2013. Study of Long-Term Variations in the Black Sea Fields Using an Interdisciplinary Physical and Biogeochemical Model. *Izvestiya, Atmospheric and Oceanic Physics*, 49(6), pp. 622-631. doi:10.1134/S0001433813060054
5. Dorofeev, V.L. and Sukhikh, L.I., 2016. Analysis of Variability of the Black Sea Hydrophysical Fields in 1993–2012 Based on the Reanalysis Results. *Physical Oceanography*, (1), pp. 33-47. doi:10.22449/1573-160X-2016-1-33-47
6. Demyshev, S.G. and Korotaev, G.K., 1992. [Numerical Energy-Balanced Model of the Baroclinic Currents in Ocean with Uneven Bottom on a C-Grid]. In: INM RAS, 1992. *Numerical Models and Results of Calibration Calculations of Currents in the Atlantic Ocean*. Moscow: Institute of Numerical Mathematics RAS, pp. 163-231 (in Russian).
7. Suslin, V.V. and Churilova, T.Ya., 2010. Simplified Method of Calculation of Spectral Diffuse Beam Attenuation Coefficient in the Black Sea Upper Layer on the Basis of Satellite Data. In: MHI, 2010. *Ekologicheskaya Bezopasnost' Pribrezhnoy i Shel'fovoy Zon i Kompleksnoe Ispol'zovanie Resursov Shel'fa* [Ecological Safety of Coastal and Shelf Zones

and Comprehensive Use of Shelf Resources]. Sevastopol: MHI. Iss. 22, pp. 47-60 (in Russian).

8. Ludwig, W., Dumont, E., Meybeck, M. and Heussner, S., 2009. River Discharges of Water and Nutrients to the Mediterranean and Black Sea: Major Drivers for Ecosystem Changes during Past and Future Decades? *Progress in Oceanography*, 80(3-4), pp. 199-217. doi:10.1016/j.pocean.2009.02.001

9. Korotaev, G.K., Oguz, T., Dorofeyev, V.L., Demyshev, S.G., Kubryakov, A.I. and Ratner, Yu.B., 2011. Development of Black Sea Nowcasting and Forecasting System. *Ocean Science*, 7(5), pp. 629-649. doi:10.5194/os-7-629-2011

10. Hersbach, H., Bell, B., Berrisford, P., Hirahara, S., Horányi, A., Muñoz-Sabater, J., Nicolas, J., Peubey, C., Radu, R. [et al.], 2020. The ERA5 Global Reanalysis. *Quarterly Journal of the Royal Meteorological Society*, 146(730), pp. 1999-2049. doi:10.1002/qj.3803

11. Taburet, G., Sanchez-Roman, A., Ballarotta, M., Pujol, M.-I., Legeais, J.-F., Fournier, F., Faugere, Y. and Dibarboure, G., 2019. DUACS DT2018: 25 Years of Reprocessed Sea Level Altimetry Products. *Ocean Science*, 15(5), pp. 1207-1224. doi:10.5194/os-15-1207- 2019

12. Dorofeev, V.L. and Korotaev, G.K., 2004. Assimilation of the Data of Satellite Altimetry in an Eddy-Resolving Model of Circulation of the Black Sea. *Physical Oceanography*, 14(1), pp. 42-56. doi:10.1023/B:POCE.0000025369.39845.c3

13. Roemmich, D., Johnson, G.C., Riser, S., Davis, R., Gilson, J., Brechner Owens, W., Garzoli, S.L., Schmid, C. and Ignaszewski, M., 2009. The Argo Program: Observing the Global Ocean with Profiling Floats. *Oceanography*, 22(2), pp. 34-43. doi:10.5670/oceanog.2009.36

14. Ivanov, V.A. and Belokopytov, V.N., 2013. *Oceanography of the Black Sea*. Sevastopol: ECOSI-Gidrofizika, 210 p. (in Russian).

15. Lima, L., Ciliberti, S.A., Aydoğdu, A., Masina, S., Escudier, R., Cipollone, A., Azevedo, D., Causio, S., Peneva, E. [et al.], 2021. Climate Signals in the Black Sea from a Multidecadal Eddy-Resolving Reanalysis. *Frontiers in Marine Science*, 8, 710973. doi:10.3389/fmars.2021.710973

16. Von Schuckmann, K., Le Traon, P.-Y., Smith, N., Pascual, A., Djavidnia, S., Gattuso, J.-P., Grégoire, M. and Nolan, G., eds., 2020. Copernicus Marine Service Ocean State Report, Issue 4. *Journal of Operational Oceanography*, 13(sup. 1), pp. S1-S172. doi:10.1080/1755876X.2020.1785097

17. Podymov, O.I., Zatsepin, A.G. and Ocherednik, V.V., 2021. Increase of Temperature and Salinity in the Active Layer of the Northeastern Black Sea from 2010 to 2020. *Physical Oceanography*, 28(3), pp. 257-265. doi:10.22449/1573-160X-2021-3-257–265

18. Dorofeyev, V.L. and Sukhikh, L.I., 2021. Features of Currents on the Black Sea Northwestern Shelf Based on the Numerical Simulation Results. *Physical Oceanography*, 28(4), pp. 426-437. doi:10.22449/1573-160X-2021-4-426-437

About the authors:

Viktor L. Dorofeev, Senior Research Associate, Marine Hydrophysical Institute of RAS (2 Kapitanskaya St., Sevastopol, 299011, Russian Federation), Ph.D. (Phys.-Math.), **ResearcherID: G-1050-2014**, viktor.dorofeev@mhi-ras.ru

Larisa I. Sukhikh, Research Associate, Marine Hydrophysical Institute of RAS (2 Kapitanskaya St., Sevastopol, 299011, Russian Federation), **ResearcherID: M-4381-2018**, l.sukhikh@gmail.com

Contribution of the co-authors:

Viktor L. Dorofeev – formulation of the problem, numerical computations, analysis of results

Larisa I. Sukhikh – numerical computations, analysis of results

The authors have read and approved the final manuscript.
The authors declare that they have no conflict of interest.